Mode stability of external cavity diode lasers

Sebastian D. Saliba,[1] Mark Junker,[1] Lincoln D. Turner,[2] and Robert E. Scholten[1,*]

[1]ARC Centre of Excellence for Coherent X-Ray Science, School of Physics, The University of Melbourne, Victoria 3010, Australia

[2]School of Physics, Monash University, Victoria 3800, Australia

*Corresponding author: scholten@unimelb.edu.au

Received 11 September 2009; revised 27 October 2009; accepted 27 October 2009; posted 28 October 2009 (Doc. ID 117011); published 1 December 2009

Mode stability is an important performance characteristic of external cavity diode lasers (ECDLs). It has been well established that the continuous mode-hop-free tuning range of a grating-feedback ECDL can be optimized by rotating the grating about a specific pivot location. We show that similar results can be obtained for other more convenient pivot locations by choosing instead the cavity length and grating location. The relative importance of the temperature stability of the diode and of the external cavity is also evaluated. We show that mechanically simple ECDL designs, using mostly standard components, can readily achieve a 35 GHz mode-hop-free tuning range at 780 nm. © 2009 Optical Society of America

OCIS codes: 140.2020, 140.3410, 140.3425, 140.3570, 140.3600.

1. Introduction

The highly controllable emission properties of external cavity diode lasers (ECDLs) make them an ideal lasing source for many experiments in optical and atomic physics [1–6]. These lasers take advantage of efficient low cost laser diodes and use frequency selective feedback to achieve narrow linewidth and tunability, typically with diffraction gratings in either the Littrow [7–9] or Littman–Metcalf configurations [10,11]. A great many mechanical implementations of the concept can be found in the literature, with emphasis on different figures of merit, such as passive stability [7], tunability [2,12], linewidth [2,4], simplicity of construction [8,13], or compactness [7,8,13,14]. Recent designs include lasers based on transmission gratings [15], volume holographic gratings [16], or ultranarrow filters [17–19]. The physical principles underlying these ECDL designs are described in early articles and reviews [3,20–22].

A problem with most designs is the competition among the dispersion of the internal diode cavity mode, the grating, and the external cavity mode. The different modal behavior of these elements with respect to variations in the temperature, cavity length, or grating angle, limits the laser frequency stability and the range over which the frequency can be tuned continuously. The maximum mode-hop-free tuning range is obtained by simultaneously rotating the grating while scanning the cavity length, so that the grating dispersion curve tracks with the external cavity frequency [12,23,24]. Correct treatment involves consideration of the translation of the grating in its plane as well as along the cavity [25,26]. Synchronized tuning is usually achieved by mounting the diffraction grating on a pivot arm rotated by a piezoelectric actuator. Previous investigations found the optimum location of the pivot, in terms of the grating parameters and external cavity length. However, the pivot location is often constrained by other factors, and, in particular, many ECDL designs rely on commercial kinematic mounts with predetermined pivot locations. The problem can be considered from the opposite perspective: given the pivot location, we show that the grating location and cavity length can be chosen to optimize the continuous tuning range. The results provide greater freedom in design, without practical reduction in performance.

We present a model of the mode stability of an ECDL that incorporates the different dispersive mechanisms. The model is tested using a popular ECDL

0003-6935/09/356692-09$15.00/0

design [13] and a versatile reconfigurable alternative. For the latter, the grating can be moved along the kinematic mount pivot arm or the cavity length can be varied to optimize the mode-hop-free tuning range. The cavity length can also be chosen such that the free spectral range (FSR) coincides with and therefore enhances microwave modulation, which can be useful for two-frequency excitation of the alkali atoms.

Measurements of the continuous tuning range and the thermal stability are in agreement with conclusions drawn from the mode stability model. We show that, with appropriate geometric and optical considerations, an ECDL can achieve a large mode-hop-free tuning range and good thermal stability, while remaining straightforward to construct and operate.

2. External Cavity Diode Laser

We consider a generic grating-feedback system, in particular, the Littrow configuration shown schematically in Fig. 1.

A. Reference Design

Two Littrow configuration lasers were used to highlight the different choices that can be made in designing an ECDL. The first is a previously published design (Fig. 2) [8,13] that is compact and readily constructed, requiring only a few simple manufactured parts. We further simplified the construction by replacing the complex fold-mirror mount with a rotatable mounting block screwed directly to the kinematic mount, as shown in Fig. 2. The laser is easy to use with stability and tuning range sufficient for laser cooling and trapping of atoms. Measured time-averaged linewidths are 120 to 300 kHz for typical operating parameters.

While the laser is adequate for many applications, some aspects could be improved. The temperature stability in particular is limited by poor conduction between the thermoelectrically cooled base, the diode, the alignment screws, and other material that define the external cavity. There is also little flexibility in choice of grating location L_g and external cavity length L_{ext}.

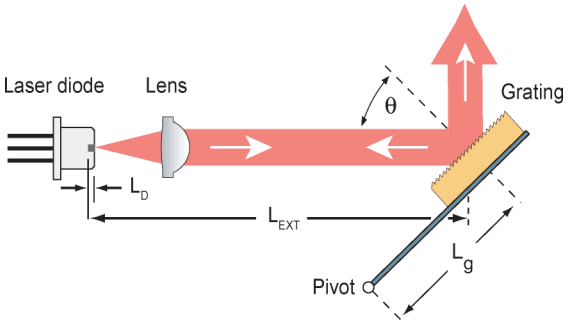

Fig. 1. (Color online) Schematic of a Littrow configuration ECDL showing a laser diode, collimation lens, and diffraction grating. θ is the Littrow angle, L_D is the diode cavity length, and L_{ext} is the external cavity length. The external cavity is formed between the rear facet of the laser diode and the diffraction grating. A single longitudinal cavity mode is selected by dispersive feedback from the grating. L_g defines the location of the grating on its pivot mount.

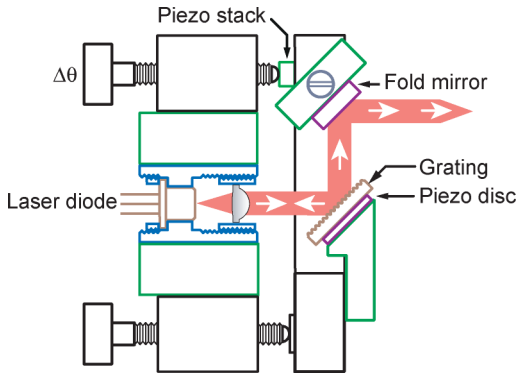

Fig. 2. (Color online) Littrow configured ECDL with a fixed output beam direction adapted with permission from C. J. Hawthorn, K. P. Weber, and R. E. Scholten, Rev. Sci. Instrum. **72**, 4477 (2001). © 2001 American Institute of Physics.

B. Split Cavity Design

Figure 3 shows an alternative ECDL that allows exploration of some of the design parameters considered here. The cavity length and grating location are readily adjustable, and the thermal coupling among the thermoelectric cooler (TEC), external cavity, and diode is greatly improved. The flexibility compromises the structural rigidity, and thus the laser is vibration sensitive and therefore more appropriate as a quickly reconfigurable prototype device rather than for practical application.

A laser diode and aspheric collimating lens ($f = 4.5$ mm, 0.55 NA) were mounted in a collimation tube inserted into a small aluminum block [27]. The

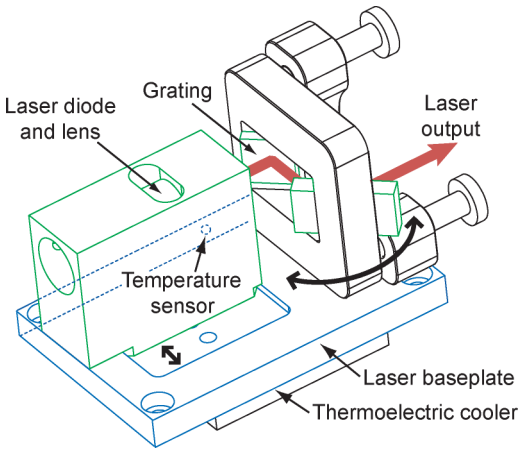

Fig. 3. (Color online) Schematic of a split-cavity ECDL used to test design variations. The laser diode block allows the collimation tube to slide inside the block, hence varying the cavity length. The grating and fold mirror are attached directly to the front plate of a modified kinematic mount, with a small piezoelectric stack to adjust the grating angle. The laser baseplate has a recess that allows translation of the laser diode block across the face of the grating for adjustment of the effective pivot point. The temperature sensor is located in the laser baseplate on the hidden side of the schematic, close to the TEC and underneath the external cavity.

grating was attached to the front face of a modified kinematic mount separated from the diode mount. A gold-coated holographic diffraction grating with 1800 grooves/mm was used, with a p-polarization diffraction efficiency of approximately 15%. A single plane mirror opposite the grating on the modified kinematic mount reflects the output beam and maintains a constant output beam direction [13]. A piezoelectric stack actuator on the horizontal axis of the grating pivot arm was used to vary the frequency by 40 GHz over the 100 V range of the stack. A 1 mm thick piezoelectric disk behind the grating provided fast frequency feedback control. The laser diode block and modified kinematic mount were attached to a separate baseplate temperature stabilized by a TEC and a thermistor. The output power for p polarization was typically 50 mW at 780 nm using a 70 mW diode. The wavelength could be tuned discontinuously over a 10 nm range by rotation of the grating alone and over a wider range with suitable temperature adjustment.

The laser diode block slides in a recess on the plate so that the beam can be centered on the grating or to match the cavity length and grating angle tuning as discussed later. The collimation tube slides into the laser diode block to allow easy variation of the external cavity length between approximately 10 and 50 mm. Additionally, the kinematic mount rotates freely relative to the diode output for grating incident angles of 30–60° without changing the output beam direction. Hence a variety of diode wavelength and grating combinations was possible, for example, gratings between 1200 and 2400 grooves/mm for a 780 nm diode or wavelengths between 637 and 1500 nm for a grating with 1200 grooves/mm. To illustrate the flexibility of the split cavity design, we investigated the advantage of variable cavity length to enhance radio frequency modulation.

C. Cavity-Amplified Microwave Modulation

Microwave modulation can be used to generate light at several different frequencies from a single ECDL, for example, to address the two atomic ground-state levels in alkali atoms [28–32]. The modulation efficiency decreases with increasing radio frequency but can be enhanced if the modulation frequency is resonant with the FSR of the external cavity [28,32]. The split cavity design (Fig. 3) is particularly convenient for applications that require current modulation to generate sidebands, because the resonant cavity length can be easily adjusted. Measurements of the efficiency of sideband production are shown in Fig. 4. A microwave signal (+10 dBm) was coupled with the dc to the diode using a bias tee. The optical power in the sidebands was measured with a 300 MHz FSR optical spectrum analyzer. The relative sideband power (Fig. 4) was observed to increase by up to 20 times when the drive frequency matched the FSR of the external cavity. The modulation efficiency increased approximately linearly with increased microwave power, with a maximum of approximately 35%. For higher input microwave powers, the laser became unstable, no longer operating in a single mode. The ability to vary the cavity length so drastically to enhance the modulation sideband signal is inherently useful and often not practical for other ECDL designs.

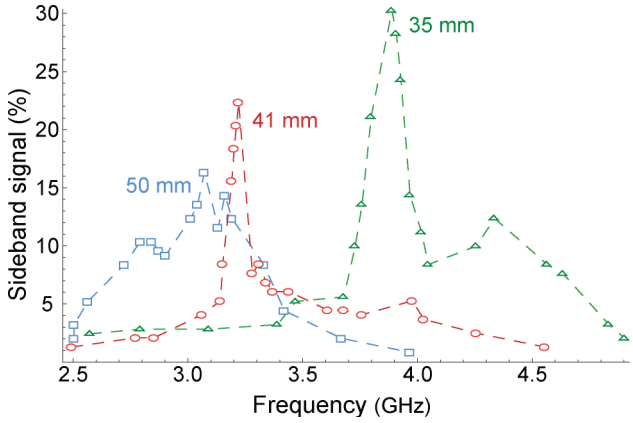

Fig. 4. (Color online) Cavity-amplified microwave modulation. Measurements show the modulation sideband peak height as a fraction of the central carrier peak height for cavity lengths of 35, 41, and 50 mm. The peaks at 3.9, 3.23, and 3.08 GHz, respectively, are in excellent agreement with the axial mode spacing condition for the effective cavity lengths.

As noted above, the split cavity laser is relatively susceptible to external vibration. Due to the extreme sensitivity of laser frequency to cavity length (25 MHz/nm for a 780 nm diode), the grating mount, which is typically adjustable to allow for laser alignment and tuning, should be rigid. In the reference design above (Fig. 2), vibrations to the diode mount and grating mount are inherently common mode, such that the diode and grating vibrate together, with comparatively little effect on the external cavity length. For the split cavity laser, the diode mount is rigid, but the grating mount is comparatively flexible, so that the cavity length and laser frequency are strongly affected by external vibration. The design was nevertheless quite useful to evaluate the effects of varying cavity length and grating offset. The thermal coupling between critical elements was also improved, enhancing the frequency stability of the laser as discussed in Subsection 3.B.1.

3. Mode Selection

Output frequency ν of a grating-feedback ECDL depends on a combination of frequency-dependent gain and loss factors: the semiconductor gain profile G_D, the grating angle and dispersion D, and the longitudinal modes of the three cavities formed between the front and the rear facets of the diode and the grating. The product of these factors is

$$T_{\text{total}} = G_D D T_D T_{\text{inner}} T_{\text{outer}}, \tag{1}$$

where T_D, T_{inner}, and T_{outer} are the transmission functions for the cavities formed between the front and the rear facets of the diode, the front diode facet and the grating, and between the rear diode facet and the grating, respectively. The laser will oscillate at

that frequency for which the product of these factors is maximum.

The relative dispersive factors are compared in Fig. 5. The intrinsic semiconductor gain profile is very broad (25 nm for a 780 nm AlGaAs laser diode) in comparison with other dispersive mechanisms in an ECDL [20]. Here we approximate the gain profile G_D as Gaussian with center frequency ν_0 and standard deviation σ. The dispersion of the diffraction grating can be evaluated from the diffracted intensity D, approximated by assuming a square-slit profile with the slit width equal to half of grating period d [33], such that

$$D = \left[\frac{\sin(kN\mathrm{d}\,\sin\theta)}{N\,\sin(kN\mathrm{d}\,\sin\theta)}\right]^2 \mathrm{sinc}^2\left(\frac{k\mathrm{d}\,\sin\theta}{2}\right), \qquad (2)$$

where θ is the Littrow angle, $k\times = 2\pi/\lambda$ is the wavenumber, and $N = 2a/d$ is the number of grooves illuminated for $1/e^2$ beam diameter $2a$. The internal diode cavity modes are described by the Airy function [33]

$$T_D = \frac{1}{1 + F\sin^2(\delta(\nu)/2)}, \qquad (3)$$

where $F = 4\sqrt{r_1 r_2}/(1-\sqrt{r_1 r_2})^2$ is the coefficient of finesse for the diode cavity, $r_{1,2}$ are the amplitude reflection coefficients of the rear and front facets, $\delta(\nu) = 4\pi n L_D \nu/c$ is the phase difference, L_D is the cavity length, and n is the refractive index. A typical $\lambda = 780$ nm single-mode laser diode [27] has a physical cavity length of $L_D = 0.25$ mm and a refractive index of $n_D = 3.5$, giving a mode spacing of $\Delta\nu = c/2L_D = 170$ GHz. The final dispersive factor for the external cavity modes is again described by Eq. (3) with the appropriate changes to reflectance amplitudes and cavity length. For a 15 mm external cavity in air the mode spacing is 10 GHz.

The combination of dispersive factors is sufficient to force single-mode operation for typical operating conditions with the laser diode running well above threshold [3,7,8]. From Fig. 5 it is clear that several external cavity modes can have similar combined gain, and thus the laser can readily jump between two cavity modes. Small changes to the intrinsic diode or external cavity mode frequencies, and even the semiconductor gain profile central frequency, can shift the relative peak heights so as to favor a different external cavity mode. Such mode hops are a critical performance limitation for many ECDL applications.

Mode instabilities can be divided into static and dynamic mode hops: dynamic, when the laser should scan through a frequency range continuously; static, when the laser is expected to operate at a single frequency.

A. Dynamic Mode Stability

It is often necessary to scan the laser frequency continuously over a range of several gigahertz, for example, through an atomic hyperfine spectrum. If the frequency is changed via the cavity length or grating angle alone, a mode hop will occur when the product of cavity mode transmission and diffraction grating dispersion falls below the gain for an adjacent external cavity mode. The mode-hop-free range can be extended by simultaneously rotating the grating and changing the cavity length. To match the grating angle tuning rate $\mathrm{d}\nu_g/\mathrm{d}\theta$ with the external cavity mode tuning rate $\mathrm{d}\nu_{\mathrm{ext}}/\mathrm{d}L_{\mathrm{ext}}$, the diffraction grating is usually mounted on a pivot arm, rotated by a multilayer piezoelectric actuator, with a tightly constrained pivot location dependent on the cavity length, grating position, and dispersion. Here we instead assume that the pivot is fixed, for example, because of the use of a standard kinematic mount for the grating [8,13], and consider how the grating position and cavity length can be adjusted to match the two tuning effects.

The external cavity mode frequency is

$$\nu_{\mathrm{ext}} = \frac{mc}{2(L_{\mathrm{ext}} - L_e)}, \qquad (4)$$

and the central diffracted frequency is

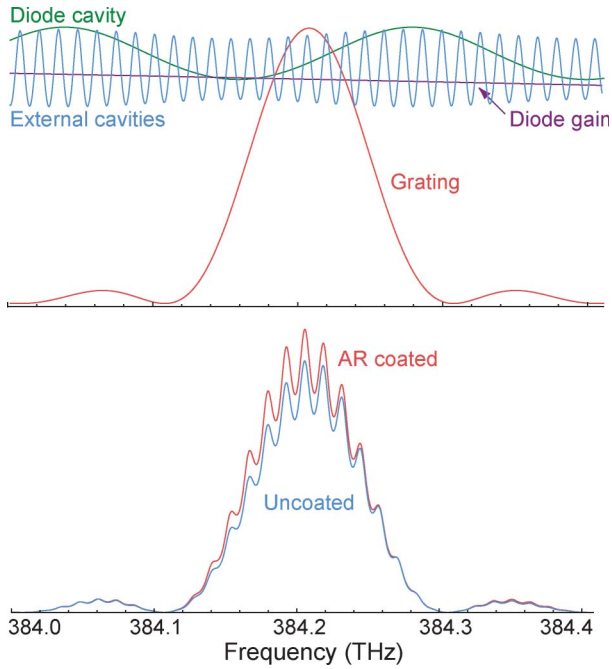

Fig. 5. (Color online) Schematic representation for the various frequency-dependent factors of an ECDL (top) calculated for $\lambda = 780$ nm, $L_D = 0.25$ mm, $n_D = 3.5$, $L_{\mathrm{ext}} = 15$ mm, $R_1 = 0.85$, and $R_2 = 0.02$. The diffracted grating intensity was calculated assuming a square-slit grating profile with a slit width equal to half of the period, a beam diameter of $2a = 2.2$ mm, and p polarization. The diode gain curve is assumed Gaussian, with a standard deviation of $\sigma = 8.5$ nm [20]. The calculated frequency responses of the combined ECDL mode spectrum for AR-coated and uncoated diodes are also shown (bottom). The grating (1800 grooves/mm), laser diode cavity mode, laser diode gain profile, and external cavity mode dispersions are all included. For the AR-coated diode, the front facet intensity reflectivity was taken to be $R_2 = 10^{-4}$.

$$\nu_g = \frac{c}{2d\sin(\theta-\theta_s)}, \tag{5}$$

where L_e is the cavity length change that is due to grating rotation θ_s. Ideally the variation of ν_{ext} and ν_g with rotation will be identical, such that the frequency mismatch $\delta\nu = \nu_g - \nu_{\text{ext}}$ remains constant and preferably small. Using the geometry of Fig. 6, which applies to several ECDL designs [8,13], we determine that

$$L_e = \frac{L_o(1-\cos\theta_s) + L_g\sin\theta_s}{\cos(\theta-\theta_s)}, \tag{6}$$

where L_g is the offset of the grating along the pivot arm and L_o is the orthogonal distance from the pivot arm to the grating face. Taking the derivative, we have

$$\frac{dL_e}{d\theta_s} = \frac{L_g\cos\theta + L_o(\sin\theta - \sin(\theta-\theta_s))}{\cos^2(\theta-\theta_s)}, \tag{7}$$

and at $\theta_s = 0$,

$$\frac{dL_e}{d\theta_s} = \frac{L_g}{\cos\theta} \tag{8}$$

as might be expected from a simple geometric consideration. The derivatives of Eqs. (4) and (5) are then

$$\frac{d\nu_{\text{ext}}}{d\theta_s} = -\frac{\nu_{\text{ext}}}{L_{\text{ext}}}\frac{L_g}{\cos\theta}, \qquad \frac{d\nu_g}{d\theta_s} = -\frac{\nu_g}{\tan\theta}. \tag{9}$$

For $\nu_{\text{ext}} = \nu_g$, we find that the tuning effects match when

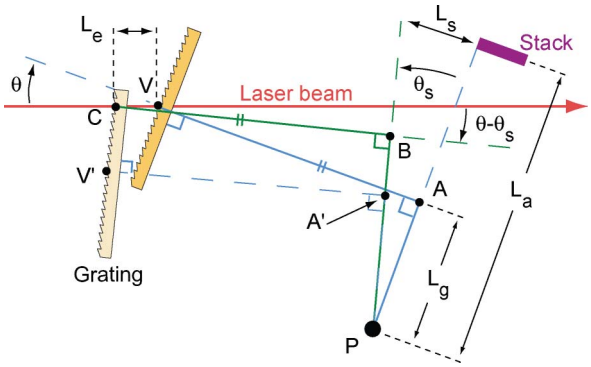

Fig. 6. (Color online) Geometry for calculating cavity length change L_e that is due to grating rotation θ_s about pivot point P caused by a piezoelectric actuator extension L_s perpendicular to the pivot arm at a distance of L_a. θ is the grating angle, AV is the distance along the grating normal from V to the pivot arm, and $PA = L_g$ is the distance along the pivot arm to AV. $\angle PA'V'$ is the rotation of $\angle PAV$ about P by angle θ_s. If the stack length increases by L_s, the laser strikes the grating at C, hence the cavity length change is $L_e = VC$. The distance from pivot arm to grating face is $L_o = AV = BC$.

$$L_{\text{ext}} = L_g\frac{\tan\theta}{\cos\theta}. \tag{10}$$

For an 1800 groove/mm grating operating at 780.2 nm, with $L_a = 38$ mm and $L_g = 15$ mm, we calculated $L_{\text{ext}} = 20.8$ mm with a mismatch of $\delta\nu < 2$ MHz over the full $L_s = \pm 2\,\mu$m 40 GHz piezoelectric stack scan, as shown in Fig. 7.

Although the matching condition is not perfect for the full scan, it is relatively insensitive to grating position and cavity length, in comparison with the critical sensitivity of the optimum pivot location for an arbitrary cavity length and grating offset [12,23,25]. As noted elsewhere [24], locating the pivot away from the perfect matching position, within specific constraints (e.g., along a line perpendicular to the grating), reduces the matched tuning range but makes the precise location less critical. Figure 8 shows the detuning mismatch versus cavity length for our geometry with a selection of fixed L_g.

1. *Experiment: Mode-Hop-Free Tuning Range*

Figure 7 shows that the grating rotation and cavity length tuning effects can be matched to within 2 MHz over a large (40 GHz) scan of the laser frequency, if the grating offset and cavity length are exactly matched to the grating arm pivot location. Even if the conditions are only approximately met, the tuning mismatch can still be well within an external cavity free spectral range for a large scan, as shown in Fig. 8, and therefore allow mode-hop-free scanning.

With the reference design (Fig. 2) for $\lambda = 780$ nm and an 1800 groove/mm grating, matching the grating angle and cavity mode tuning rate is well approximated by the condition $L_{\text{ext}} = \sqrt{2}L_g$. This can be achieved by adjusting the position of the grating along the pivot arm of the kinematic mount or by adjusting the cavity length. Typically, $L_g = 15$ mm and the optimal cavity length is then $L_{\text{ext}} = 20.8$ mm. However, the design does not allow simple adjustment of the cavity length and grating offset, and so we investigated optimization of the continuous tuning range using the split cavity laser.

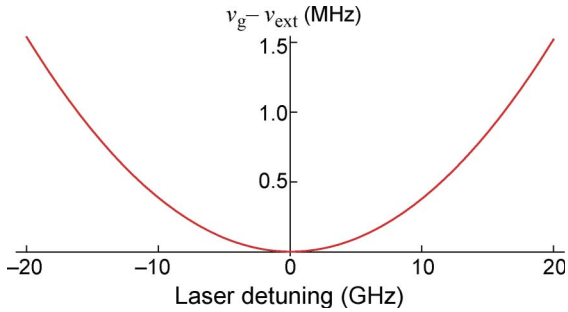

Fig. 7. (Color online) Tuning mismatch between grating and cavity mode frequencies $\delta\nu = \nu_g - \nu_{\text{ext}}$ as the grating is rotated by a piezoelectric actuator at $L_a = 38$ mm from the pivot, grating offset of $L_g = 15$ mm, and matched cavity length $L_{\text{ext}} = L_g\tan\theta/\cos\theta = 20.8$ mm. The piezo actuator extension range of $L_s = \pm 2\,\mu$m changes the laser frequency by ± 20 GHz.

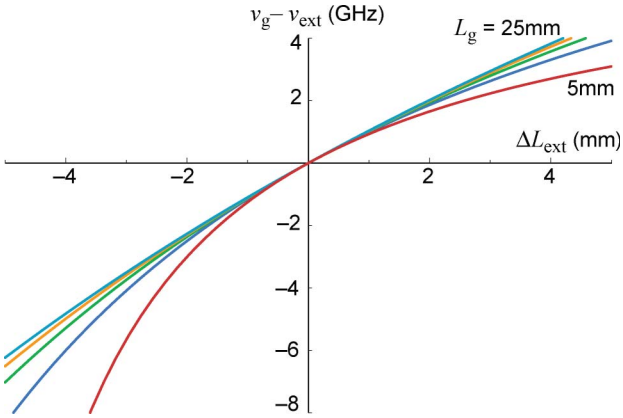

Fig. 8. (Color online) Maximum tuning mismatch for a change in laser frequency of 20 GHz for different errors in cavity length ΔL_{ext} relative to the optimum. $L_a = 38$ mm, $L_g = 5$ to 25 mm in 5 mm steps.

The laser frequency was scanned with a sinusoidal signal driving the piezoelectric stack and measured with a Fizeau wavemeter [27]. The amplitude of the sinusoid and thus the width of the frequency scan was increased until a mode hop was observed. The results are plotted in Fig. 9 as the maximum frequency range over which the laser could be scanned without a mode hop, divided by the FSR for that cavity length, for a range of cavity lengths around the optimum.

Results were obtained with a standard 780 nm laser diode [27] and also with the same type of diode with an additional antireflection (AR) coating to reduce the influence of the internal diode cavity. The continuous tuning ranges were typically 8 GHz (just over 1 FSR) and 16 GHz (2.5 FSR), respectively, with fixed injection currents of 88 and 90 mA.

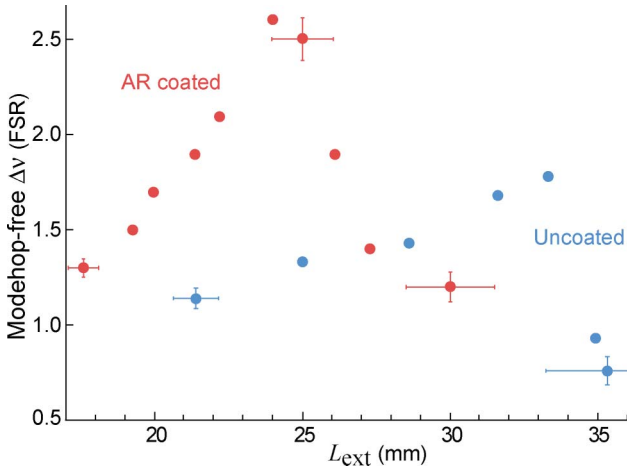

Fig. 9. (Color online) Mode-hop-free tuning range for the split cavity laser with standard and AR-coated diodes at fixed injection currents (88 and 90 mA) for a range of cavity lengths. The tuning range is clearly enhanced by appropriate adjustment of the external cavity length for a given grating pivot location: $L_a = 38$ mm and grating offset $L_g = 15$ mm from the pivot. The cavity length was determined from a measure of the cavity free spectral range (FSR), obtained by scanning the diode current and observing the change in laser frequency as the laser mode hopped to the adjacent longitudinal cavity mode. The uncertainty bars were derived from the estimated accuracy of ±0.25 GHz in determining the maximum mode-hop-free range and FSR and propagating that to the calculated cavity length.

The overall cavity length can be dynamically corrected as the laser frequency is changed by adding an injection current bias proportional to the piezo voltage. Typically −0.3 to −1.0 mA/GHz will ensure that the cavity mode follows the grating mode more precisely. With current bias, the continuous tuning range increased to 24 GHz (4 FSR) for the standard diode and more than 35 GHz with the coated diode; the latter was limited by the range of current bias (30 mA). With increased current bias and more precise matched tuning, up to 90 GHz has been achieved without special coatings [34–36].

2. *Conclusion: Dynamic Mode Stability*

In summary, we emphasize that in many cases the mode-hop-free tuning range can be dramatically increased by simply adjusting the cavity length, or, if the length is constrained by the need to enhance microwave modulation, by positioning the grating at the optimum location on its mount. Matching the grating angle and external cavity mode tuning rates allows mode-hop-free scan ranges several times the external cavity FSR. The continuous tuning range can be extended by applying a suitable injection current bias.

B. Static Mode Stability

The static mode stability of an ECDL is affected by the ambient air pressure and temperature. The air pressure affects the optical path length of the external cavity, and local atmospheric pressure variations can cause frequency drifts of several hundred megahertz per hour for a 15 mm external cavity [37]. The effect of pressure fluctuations can be reduced or eliminated by hermetically sealing the ECDL cavity, which is helpful to remove the large frequency excursions (hundreds of megahertz) caused by walking briskly past an ECDL. Frequency drifts can also be compensated with active feedback to the cavity length.

Temperature-dependent effects on the laser frequency, which can be more problematic, occur through three main processes. First, the optical path length of the diode cavity varies with temperature due to thermal expansion, given by $dL_D/dT = k_D L_D$, where k_D is the thermal expansion coefficient and L_D is the initial length of the diode. For small temperature changes, the diode cavity mode changes as $d\nu/dT = \nu_0 k_D$, where ν_0 is the initial frequency. For a 780 nm diode with $k_D = 5 \times 10^{-6}$/K, $d\nu/dT = -1.9$ GHz/K due to thermal expansion alone. The refractive index and hence optical path length also changes with temperature, and the combined tuning rate is −30 GHz/K [3].

The diode temperature is affected by the external temperature of the diode package and also by the injection current that is due to resistive heating. The injection current also directly controls the charge

carrier density, which in turn affects the index of refraction and thus the optical path length of the cavity. The combined sensitivity to injection current is around $-3\,\mathrm{MHz}/\mu\mathrm{A}$ at low frequencies [3,37].

The second temperature effect is variation of the frequency of the gain peak of the semiconductor, again due to thermal expansion, in this case semiconductor lattice spacing. The lattice spacing affects the bandgap energy and hence the peak gain frequency. The shift is approximately $-125\,\mathrm{GHz/K}$ [3].

The third and usually most important effect is thermal expansion of the external cavity. In an ECDL the laser frequency selection is dominated by the external cavity mode at $\nu = mc/2L_{\mathrm{ext}}$, where ν is the frequency of mode m for a given cavity length L_{ext}. For an aluminum cavity with $k_{Al} = 20 \times 10^{-6}/\mathrm{K}$, the temperature sensitivity at 780 nm is $d\nu/dT = -7.68\,\mathrm{GHz/K}$.

Although this appears to be the smallest of the three effects, the other variations are effectively zero provided they are not sufficient to cause the laser to mode hop. The laser will mode hop when the product in Eq. (1) is maximized in an adjacent external cavity mode. A small change in external cavity length directly changes the laser frequency, whereas drift of the diode cavity mode frequency, and/or the diode gain peak frequency, must accumulate until there is a mode hop to an adjacent cavity mode. For a 15 mm external cavity the limit is $\sim \mathrm{FSR}/2 = 5\,\mathrm{GHz}$ (equivalent to $\approx 0.6\,\mathrm{K}$). Provided the laser diode thermal stability is adequate to maintain the diode frequency within this range, the external cavity will still determine the output laser frequency. From the coefficients given above, the required thermal stability is approximately 0.1 K for the diode mode and 0.04 K for the gain profile.

For the external cavity, any temperature change will directly affect the frequency. Temperature control to within 0.1 mK is needed to achieve passive frequency stability of better than 1 MHz. If the laser frequency is actively stabilized to an external reference, the requirements are less stringent, but in practice millikelvin stability is still needed such that the laser can be tuned to the desired locked frequency.

For an ECDL with an AR-coated diode, the diode cavity resonance is suppressed by the dominant external cavity feedback. However, the diode cavity length change will still affect the total cavity length and hence the external cavity frequency, according to

$$\frac{d\nu}{dT} = \nu_0 \frac{L_D k_D + L_{\mathrm{ext}} k_{Al}}{L_D + L_{\mathrm{ext}}}. \tag{11}$$

For $L_D = 0.25\,\mu\mathrm{m}$ and $L_{\mathrm{ext}} = 15\,\mathrm{mm}$, $d\nu/dT$ is reduced to $d\nu/dT = 7.36\,\mathrm{GHz/K}$. The diode adds approximately 6% to the total cavity length but accounts for even less of the temperature induced frequency change that is due to the low thermal expansion coefficient of AlGaAs relative to aluminum.

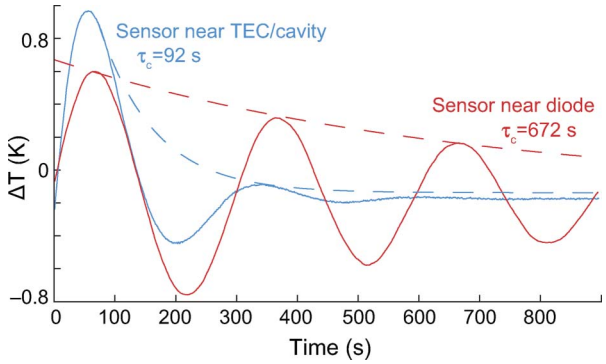

Fig. 10. (Color online) Temperature fluctuations for a sensor position close to the diode (<5 mm) results in persistent small scale oscillations. A sensor close to the TEC/external cavity responds more slowly to temperature fluctuations at the diode (25 mm away), yet the proximity to the TEC (<5 mm) and external cavity provides better thermal stability. The time constants were calculated by fitting an exponential decay to the oscillation peaks.

1. *Experiment: Thermal Stability*

ECDL designs usually focus on keeping the laser diode temperature stable at the expense of external cavity stability [8,13], although the use of two stages of temperature control to improve thermal stability has also been suggested [3]. Designs in which the diode, collimation optics, and grating are fixed within the same standard kinematic mount, as in the reference design above, are compact and easily constructed but suffer from poor thermal coupling between the ECDL components and the large thermal drifts of output frequency. By positioning the temperature sensor close to the external cavity rather than the diode (see Fig. 3), we observed a significant improvement in thermal stability. The measured temperature stability in Fig. 10 shows the temperature set-point convergence of a diode-sensor ECDL in comparison with a cavity-sensor ECDL. The temperature response is relatively fast, which allows greater gain in the temperature

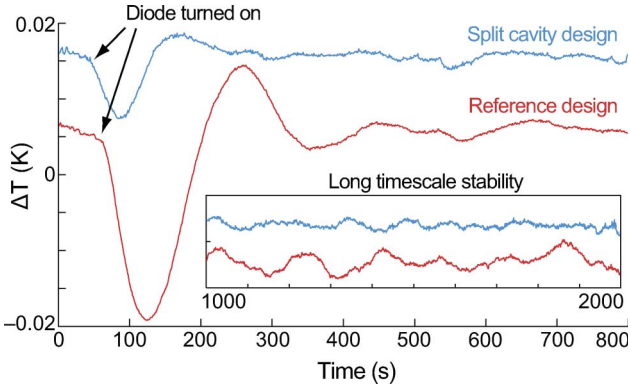

Fig. 11. (Color online) Comparison of the temperature response to a sudden change (diode turned on) in the reference design [13] and the split cavity design. Inset: a comparison of the temperature stability over a long time scale from 1000 to 2000 s. The temperature variances were $\mathrm{Var}(T) = 1.21 \times 10^{-6}\,\mathrm{K}$ and $\mathrm{Var}(T) = 3.55 \times 10^{-7}\,\mathrm{K}$.

controller and therefore improved temperature stability. The split-cavity design also improves the thermal coupling between the TEC and the laser diode. A comparison of short and long time scale temperature stability for the two designs indicates an improvement of the rms temperature stability by a factor of 2 (Fig. 11).

2. *Conclusion: Static Mode Stability*

Isolation of an ECDL from the environment is generally helpful in improving the static mode stability, for example, by hermetically sealing the laser cavity against pressure fluctuations and thermally insulating the laser, even with a simple cover. We emphasize that the dominant temperature effect on the frequency of an ECDL is thermal expansion of the (typically) aluminum external cavity and further stress the importance of stabilizing the external cavity temperature and length rather than prioritizing the diode temperature.

4. Conclusion

External cavity diode lasers offer compact, efficient, and versatile light sources for experiments in atomic physics and spectroscopy more generally. The broad gain bandwidth of the semiconductor medium offers a large wavelength tuning range, in many cases tens of nanometers, but competition among the dispersion of the internal diode cavity mode, the grating, and the external cavity mode leads to discontinuities or mode hops. The static and dynamic stability depend on free parameters of the design, such as the cavity length, the position of the diffraction grating, or the location of a temperature sensor. We have described a simple model of the mode stability and have shown that, even when the grating pivot location is constrained, the grating location and the cavity length can be chosen to optimize the continuous tuning range. Large mode-hop-free scans, up to 35 GHz or more, can be obtained without requiring a custom kinematic grating mount. The relative importance of the temperature sensitivity of the diode and of the external cavity was also considered. We emphasize that long-term laser frequency stability is primarily dependent on the cavity thermal stability, which is optimized by locating the temperature sensor near both the thermoelectric cooling device and the external cavity support rather than near the diode.

By considering these factors and especially the importance of the external cavity in determining the laser frequency, frequency-stable ECDLs with a large continuous tuning range can be constructed mostly from standard components.

References

1. M. W. Fleming and A. Mooradian, "Spectral characteristics of external-cavity controlled semiconductor lasers," IEEE J. Quantum Electron. **17**, 44–59 (1981).
2. R. Wyatt and W. J. Devlin, "10 kHz linewidth 1.5 μm InGaAsP external cavity laser with 55 nm tuning range," Electron. Lett. **19**, 110–112 (1983).
3. C. E. Wieman and L. Hollberg, "Using diode lasers for atomic physics," Rev. Sci. Instrum. **62**, 1–20 (1991).
4. K. B. MacAdam, A. Steinbach, and C. Wieman, "A narrow-band tunable diode laser system with grating feedback, and a saturated absorption spectrometer for Cs and Rb," Am. J. Phys. **60**, 1098–1111 (1992).
5. K. G. Libbrecht, R. A. Boyd, P. A. Willems, T. L. Gustavson, and D. K. Kim, "Teaching physics with 670 nm diode lasers-construction of stabilized lasers and lithium cells," Am. J. Phys. **63**, 729–737 (1995).
6. C. P. Pearman, C. S. Adams, S. G. Cox, P. F. Griffin, D. A. Smith, and I. G. Hughes, "Polarization spectroscopy of a closed atomic transition: applications to laser frequency locking," J. Phys. B **35**, 5141–5151 (2002).
7. L. Ricci, M. Weidemüller, T. Esslinger, A. Hemmerich, C. Zimmermann, V. Vuletic, W. König, and T. W. Hänsch, "A compact grating-stabilized diode laser system for atomic physics," Opt. Commun. **117**, 541–549 (1995).
8. A. S. Arnold, J. S. Wilson, and M. G. Boshier, "A simple extended-cavity diode laser," Rev. Sci. Instrum. **69**, 1236–1239 (1998).
9. T. Hof, D. Fick, and H. J. Jänsch, "Application of diode lasers as a spectroscopic tool at 670 nm," Opt. Commun. **124**, 283–286 (1996).
10. K. C. Harvey and C. J. Myatt, "External-cavity diode laser using a grazing-incidence diffraction grating," Opt. Lett. **16**, 910–912 (1991).
11. S. Lecomte, E. Fretel, G. Mileti, and P. Thomann, "Self-aligned extended-cavity diode laser stabilized by the Zeeman effect on the cesium D_2 line," Appl. Opt. **39**, 1426–1429 (2000).
12. W. R. Trutna, Jr., and L. F. Stokes, "Continuously tuned external cavity semiconductor laser," J. Lightwave Technol. **11**, 1279–1286 (1993).
13. C. J. Hawthorn, K. P. Weber, and R. E. Scholten, "Littrow configuration tunable external cavity diode laser with fixed direction output beam," Rev. Sci. Instrum. **72**, 4477–4479 (2001).
14. V. V. Vassiliev, S. Zibrov, and V. Velichansky, "Compact extended-cavity diode laser for atomic spectroscopy and metrology," Rev. Sci. Instrum. **77**, 013102 (2006).
15. M. Merimaa, H. Talvitie, P. Laakkonen, M. Kuittinen, I. Tittonen, and E. Ikonen, "Compact external-cavity diode laser with a novel transmission geometry," Opt. Commun. **174**, 175–180 (2000).
16. T. Hieta, M. Vainio, C. Moser, and E. Ikonen, "External-cavity lasers based on a volume holographic grating at normal incidence for spectroscopy in the visible range," Opt. Commun. **282**, 3119–3123 (2009).
17. P. Zorabedian and W. R. Trutna, Jr., "Interference-filter-tuned, alignment-stabilized, semiconductor external-cavity laser," Opt. Lett. **13**, 826–828 (1988).
18. X. Baillard, A. Gauguet, S. Bize, P. Lemonde, P. Laurent, A. Clairon, and P. Rosenbusch, "Interference-filter-stabilized external-cavity diode lasers," Opt. Commun. **266**, 609–613 (2006).
19. M. Gilowski, C. Schuberta, M. Zaisera, W. Herra, T. Wübbenaa, T. Wendricha, T. Müllera, E. M. Rasela, and W. Ertmer, "Narrow bandwidth interference filter-stabilized diode laser systems for the manipulation of neutral atoms," Opt. Commun. **280**, 443–447 (2007).
20. P. Zorabedian, "Tunable external-cavity semiconductor lasers," in *Tunable Lasers Handbook*, F. J. Duarte, ed. (Academic, 1995), pp. 349–442.
21. G. Galbács, "A review of applications and experimental improvements related to diode laser atomic spectroscopy," Appl. Spectrosc. Rev. **41**, 259–303 (2006).

22. B. Mroziewicz, "External cavity wavelength tunable semiconductor lasers: a review," Opto-Electron. Rev. **16**, 347–366 (2008).
23. P. McNicholl and H. J. Metcalf, "Synchronous cavity mode and feedback wavelength scanning in dye laser oscillators with gratings.," Appl. Opt. **24**, 2757–2761 (1985).
24. L. Nilse, J. J. Davies, and C. S. Adams, "Synchronous tuning of extended cavity diode lasers: the case for an optimum pivot point," Appl. Opt. **38**, 548–553 (1999).
25. M. de Labachelerie and G. Passedat, "Mode-hop suppression of Littrow grating-tuned lasers," Appl. Opt. **32**, 269–274 (1993).
26. M. de Labachelerie, H. Sasada, and G. Passedat, "Mode-hop suppression of Littrow grating-tuned lasers: erratum," Appl. Opt. **33**, 3817–3819 (1994).
27. We used a Thorlabs LT230P-B collimation tube, Newport Ultima and Fine-Adjustment Earth-series kinematic mounts, Spectraphysics 33001FL02-330H gold-coated holographic grating, Melcor CP1.4-71-045L TEC, Tokin AE0203D04 piezoelectric actuator, Sanyo DL-7140-201 diode, High Finesse WS-6 Fizeau wavemeter, and a MOGLabs DLC-202 ECDL controller. Note: certain commercial equipment, instruments, or materials are identified in this paper in order to adequately specify the experimental procedure. Such identification does not imply recommendation or endorsement, nor does it imply that the materials or equipment are necessarily the best available for the purpose.
28. C. J. Myatt, N. R. Newbury, and C. E. Wieman, "Simplified atom trap by using direct microwave modulation of a diode laser," Opt. Lett. **18**, 649–651 (1993).
29. P. Feng and T. Walker, "Inexpensive diode laser microwave modulation for atom trapping," Am. J. Phys. **63**, 905–908 (1995).
30. J. Ringot, Y. Lecoq, J. C. Garreau, and P. Szriftgiser, "Generation of phase-coherent laser beams for Raman spectroscopy and cooling by direct current modulation of a diode laser," Eur. Phys. J. D **7**, 285–288 (1999).
31. R. Kowalski, S. Root, S. D. Gensemer, and P. L. Gould, "A frequency-modulated injection-locked diode lsaer for two-frequency generation," Rev. Sci. Instrum. **72**, 2532–2534 (2001).
32. A. Waxman, M. Givon, G. Aviv, D. Groswasser, and R. Folman, "Modulation enhancement of a diode laser in an external cavity," Appl. Phys. B **95**, 301–305 (2009).
33. M. Born and E. Wolf, *Principles of Optics*, 6th ed. (Pergamon, 1993), pp. 402–405.
34. T. Nayuki, T. Fujii, K. Nemoto, M. Kozuma, M. Kourogi, and M. Ohtsu, "Continuous wavelength sweep of external cavity laser diode without antireflection coating on output facet," Opt. Rev. **5**, 267–270 (1998).
35. C. Petridis, I. D. Lindsay, D. J. M. Stothard, and M. Ebrahimzadeh, "Mode-hop-free tuning over 80 GHz of an extended cavity diode laser without antireflection coating," Rev. Sci. Instrum. **72**, 3811–3815 (2001).
36. J. Hult, I. S. Burns, and C. F. Kaminski, "Wide-bandwidth mode-hop-free tuning of extended-cavity GaN diode lasers," Appl. Opt. **44**, 3675–3685 (2005).
37. H. Talvitie, A. Pietiläinen, H. Ludvigsen, and E. Ikonen, "Passive frequency and intensity stabilization of extended-cavity diode lasers," Rev. Sci. Instrum. **68**, 1–7 (1997).